

1 **The Promise of Deep Learning for BCIs: Classification of** 2 **Motor Imagery EEG using Convolutional Neural Network**

3

4 Navneet Tibrewal¹, Nikki Leeuwis^{1,2}, Maryam Alimardani¹

5 ¹Department of Cognitive Science and Artificial Intelligence, Tilburg University,

6 ²Research Department, Unravel Research, Burgermeester Reigerstraat 78, 3581 KW

7 Utrecht, The Netherlands

8 Corresponding author: Maryam Alimardani, m.alimardani@tilburguniversity.edu

9

10 **Abstract**

11 Motor Imagery (MI) is a mental process by which an individual rehearses body
12 movements without actually performing physical actions. Motor Imagery Brain-
13 Computer Interfaces (MI-BCIs) are AI-driven systems that capture brain activity
14 patterns associated with this mental process and convert them into commands for
15 external devices. Traditionally, MI-BCIs operate on Machine Learning (ML)
16 algorithms, which require extensive signal processing and feature engineering to
17 extract changes in sensorimotor rhythms (SMR). However, in recent years, Deep
18 Learning (DL) models have gained popularity for EEG classification as they provide a
19 solution for automatic extraction of spatio-temporal features in the signals. In this
20 study, EEG signals from 54 subjects who performed a MI task of left- or right-hand
21 grasp was employed to compare the performance of two MI-BCI classifiers; a ML
22 approach vs. a DL approach. In the ML approach, Common Spatial Patterns (CSP)
23 was used for feature extraction and then Linear Discriminant Analysis (LDA) model
24 was employed for binary classification of the MI task. In the DL approach, a
25 Convolutional Neural Network (CNN) model was constructed on the raw EEG

CNN Classification for Motor Imagery BCIs

26 signals. The mean classification accuracies achieved by the CNN and CSP+LDA
27 models were 69.42% and 52.56%, respectively. Further analysis showed that the DL
28 approach improved the classification accuracy for all subjects within the range of 2.37
29 to 28.28% and that the improvement was significantly stronger for low performers.
30 Our findings show promise for employment of DL models in future MI-BCI systems,
31 particularly for BCI inefficient users who are unable to produce desired sensorimotor
32 patterns for conventional ML approaches.

33

34 **Keywords: motor imagery (MI), brain-computer interface (BCI), artificial**
35 **intelligence (AI), EEG, machine learning (ML), deep learning (DL),**
36 **convolutional neural network (CNN), linear discriminant analysis (LDA), BCI**
37 **inefficiency**

CNN Classification for Motor Imagery BCIs

38 **1 Introduction**

39 Motor Imagery (MI) is a dynamic experience where the user contemplates mental
40 imagination of motor movement without activation of any muscle or peripheral nerve.
41 A Motor Imagery Brain-Computer Interface (MI-BCI) serves as a system that
42 converts brain signals generated during such imagination into an actionable sequence
43 ([Alimardani et al., 2018](#); [Cho et al., 2018](#); [Millán et al., 2010](#); [Pfurtscheller & Neuper,](#)
44 [2001](#))
45 MI-BCI systems mainly utilize electroencephalogram (EEG) for measurement of
46 brain activity ([Lebedev & Nicolelis, 2017](#)). EEG provides high temporal resolution,
47 can be portable, is relatively low cost and represents synchronous electrical signals
48 produced by the brain ([Lebedev & Nicolelis, 2017](#)). However, the recorded EEG
49 signals are non-stationary and suffer from a low signal-to-noise ratio (SNR) and poor
50 spatial resolution. Therefore, in order to employ them in a BCI system, it is necessary
51 to apply advanced signal processing techniques to clean the data from artefacts and
52 extract relevant spatial, temporal and frequency information from the signals for the
53 classification problem ([Bharne & Kapgate, 2014](#)).
54 Traditionally, MI-BCIs operate on machine learning (ML) algorithms in which spatial
55 features associated with movement imagination are recognized. The imagining of a
56 left or right body movement is accompanied by a lateralization of event-related
57 (de)synchronization (ERD/ERS) in the mu (7-13 Hz) and beta (13-30 Hz) frequency
58 bands of EEG signals ([Pfurtscheller et al., 2006](#); [Avanzini et al., 2012](#); [Barros & Neto,](#)
59 [2018](#); [Wang et al., 2019](#)). This brain activity feature serves as an input to the ML
60 algorithm classifying the imagined body movements. Therefore, the system relies on
61 the user to consciously modulate their brain activity such that the lateralization can be
62 detected. It is shown that fifteen to thirty percent of users cannot accomplish

CNN Classification for Motor Imagery BCIs

63 distinctive brain waves such that the classifier reaches accuracy above 70%. This is
64 called ‘*BCI illiteracy*’ ([Allison & Neuper, 2010](#)) or ‘*BCI inefficiency*’ ([Thompson,](#)
65 [2019](#)), where a user is considered unable to control a BCI, even after extensive
66 training. But the issue of BCI inefficiency might be argued more nuanced, as
67 successful BCI control depends on a synergy between man and machine, and
68 therefore enhancements on both sides are needed to reach efficient control
69 ([Thompson, 2019](#)).

70 In almost half of MI-BCI studies ([Wierzgala et al., 2018](#)), the mu suppression
71 lateralization is picked up by the Common Spatial Pattern (CSP) algorithm that
72 linearly transforms EEG data into a subspace with a lower dimension in which the
73 variance of one class (the imagined side) is maximized while the variance of the other
74 class is minimized ([Khan et al., 2019](#); [Shen et al., 2017](#)). The output of the CSP filter
75 is then used as an input for a ML algorithm, such as linear discriminant analysis
76 (LDA), support vector machine (SVM), or logistic regression (LR) to distinguish
77 EEG patterns associated with motor imageries ([Miao et al., 2020](#)). LDA is a very
78 popular model for binary classification of the MI task ([Yuksel & Olmez, 2015](#)); it
79 works on the concept of minimizing the ratio of within-class scatter to between-class
80 scatter while keeping the intrinsic details of the data intact ([Shashibala & Gawali,](#)
81 [2016](#)). Hence, LDA creates a hyperplane in the feature space based on evaluation of
82 the training data to maximize the distance between the two classes and minimize the
83 variance of the same class ([Aydemir & Kayikcioglu, 2013](#); [Hasan et al., 2015](#)).

84 Although, ML techniques are commonly used for binary classification of MI-BCIs
85 systems, they are extremely vulnerable to variability between subjects and drifts in the
86 brain signals ([Millán et al, 2010](#)). ML techniques do not work well under the
87 influence of noise and outliers, which are difficult to segregate from the primary data

CNN Classification for Motor Imagery BCIs

88 ([Müller et al., 2004](#)). Additionally, the performance of ML classifiers is highly
89 dependent on the type of feature extraction technique that is used ([Hsu, 2010](#)). More
90 importantly, they suffer from the ‘*curse of dimensionality*’ and are therefore highly
91 susceptible to overfitting ([AlZoubi et al., 2008](#)). The curse of dimensionality stems
92 from an imbalance between the number of extracted features and the number of
93 training EEG patterns (i.e. number of subjects). In order to extract relevant
94 information from the EEG data, multiple feature extraction techniques are adopted,
95 which add more and more dimensions to the feature space ([AlZoubi et al., 2008](#); [Lotte](#)
96 [et al., 2018](#)). This creates a situation in which the features vastly outnumber the
97 observations, resulting in overfitting and an erroneous model performance. Therefore,
98 ML approaches require yet another step of feature selection for reduction of
99 dimensionality in the training data, which yields additional computational costs in
100 terms of memory usage and CPU time.

101 Deep Learning (DL) classifiers are a promising alternative to address the complexity
102 of EEG signals, as they can work with raw data and directly learn features and capture
103 structure of a large dataset without any feature engineering or selection processes
104 ([Albawi et al., 2018](#); [Robinson et al., 2019](#); [Wang et al., 2018](#); [Yang et al., 2015](#)).

105 Thus, the issue of information loss while generating and selecting features is avoided
106 when DL classifiers are used ([Qiao & Bi, 2019](#)). Additionally, they can be used to
107 stabilize the learning process by overcoming the issue of noise and outliers in the data
108 ([Al-Ani et al., 2010](#)). DL generates high-level abstract features from low-level
109 features by identifying distributed patterns in the acquired data. Hence, DL models
110 hold the potential of handling complex and non-linear high dimensional data ([Wang et](#)
111 [al., 2019](#)).

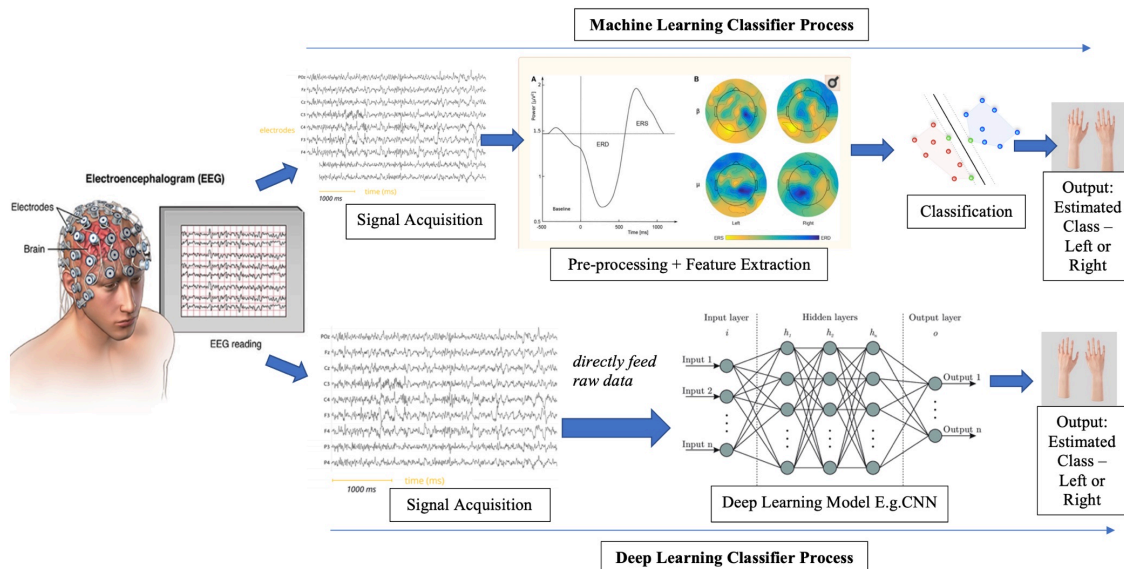
CNN Classification for Motor Imagery BCIs

112 Past research has already established the effectiveness of the DL approach, especially
113 Convolutional Neural Network (CNN), in classification of MI-EEG ([Tang et al.,](#)
114 [2017](#); [Gao et al., 2018](#); [Sakhavi et al., 2015](#); [Li et al., 2020](#); [Dai et al., 2019](#); [Tayeb et](#)
115 [al., 2019](#); [Stieger et al., 2020](#); [Zhang et al., 2021](#); [Ko et al., 2020](#); [Mane et al., 2020](#)).
116 The advantages of CNN model include handling raw data without any feature
117 engineering process, facilitating end-to-end learning and requiring lesser parameters
118 than other deep neural networks ([Shen et al., 2017](#); [Albawi et al., 2018](#)). CNN works
119 well with large datasets and can exploit the hierarchical structure in natural signals
120 ([Schirrneister et al., 2017](#)). Moreover, CNN has good regularization and degree of
121 translation invariance properties along with the ability to capture spatial and temporal
122 dependencies of EEG signals ([Aggarwal & Chugh, 2019](#)). CNN can be particularly
123 useful in classification of MI-EEG for low aptitude users. Stieger et al. ([2020](#)) showed
124 a negative correlation between online (ML-based) performance and improvement of
125 accuracy with CNN, which suggests that BCI inefficient users may benefit from
126 applying a DL classifier, even more than high aptitude users. They further showed
127 that the low performing users in the online classification did not necessarily produce
128 the expected SMR activity during MI process, but instead produced differentiating
129 activity over brain regions outside the motor cortex such as occipital and frontal
130 gamma power, which could not be recognized by CSP. Therefore, DL methods might
131 be beneficial in improving performance for inefficient users and serve as a promising
132 tool in enhancing overall BCI usability.

133 This study aims to compare the two approaches of ML and DL in classification of MI
134 EEG signals in a large group of 54 subjects. In most of previous studies, CNN has
135 been compared with ML classifiers other than CSP+LDA. However, the use of
136 CSP+LDA model is widespread in binary MI-BCI classification ([Lotte et al., 2018](#);

CNN Classification for Motor Imagery BCIs

137 [Nicolas-Alonso & Gomez-Gil, 2012](#); [Selim et al., 2018](#)). Hence, in this study, for
138 every subject, a CNN model (DL approach) was trained and its performance was
139 compared with the conventional CSP+LDA model (ML approach).
140 [Figure 1](#) shows sequential steps that were taken in each approach to construct a MI-
141 BCI classifier and obtain classification performances. The ‘*Signal Acquisition*’ step
142 was carried out through EEG to monitor the brain signals arising from the mental
143 image of the movement by the user. The complexity of the ML approach arises with
144 the steps involved in ‘*Pre-processing*’ and ‘*Feature Extraction*,’ whereas in the DL
145 approach, raw data can directly be fed into the model. Hence, by applying both
146 approaches to the data from 54 subjects, this study intends to answer the following
147 research question: “*Can a CNN classifier trained with raw EEG signals achieve a*
148 *higher performance than a machine learning model that runs on processed EEG*
149 *features for classification of a two-class Motor Imagery task?*”



150
151 **FIGURE 1** | An overview of MI-BCI classification using machine learning vs. deep
152 learning approaches. In ML approach, EEG signals are first pre-processed and
153 relevant features are extracted before applying a classifier. In DL approach, raw
154 signals are directly fed into the model.

CNN Classification for Motor Imagery BCIs

155 **2 Methods**

156 In order to compare conventional ML models with a DL approach in a large group of
157 novice BCI users, EEG signals were collected from 57 subjects while they performed
158 the MI task using an existing BCI system. Thereon, the recorded EEG signals were
159 used to train a CNN and CSP+LDA model to conduct an offline classification of two-
160 class MI task. The following section gives a description of the data collection
161 procedure and details of the classification models.

162

163 **2.1 Experiment**

164 **2.1.1 Participants**

165 In this experiment, 57 subjects participated (21 male, 36 female, $M_{age} = 20.71$, $SD_{age} =$
166 3.52). All of them were right-handed and novice to BCI and the MI task. The
167 Research Ethics Committee of Tilburg School of Humanities and Digital Sciences
168 approved the study (REDC #20201003). All subjects received explanation regarding
169 experiment procedure and signed a consent form before the experiment.

170 **2.1.2 EEG Acquisition**

171 Sixteen electrodes recorded EEG signals from the sensorimotor area according to the
172 10-20 international system (F3, Fz, F4, FC1, FC5, FC2, FC6, C3, Cz, C4, CP1, CP5,
173 CP2, CP6, T7, T8). The right earlobe was used as a reference electrode and a ground
174 electrode was set on AFz. Conductive gel was applied to keep the impedance of the
175 electrodes below 50 kOhm. Subjects were instructed to sit calmly and avoid
176 movements and excessive blinking. The signals were amplified by a g.Nautilus
177 amplifier (g.tec Medical Engineering, Austria). The data was sampled at 250
178 samples/second. The noise during EEG recording was reduced by applying a 48-52
179 Hz notch filter and 0.5-30 Hz bandpass filter.

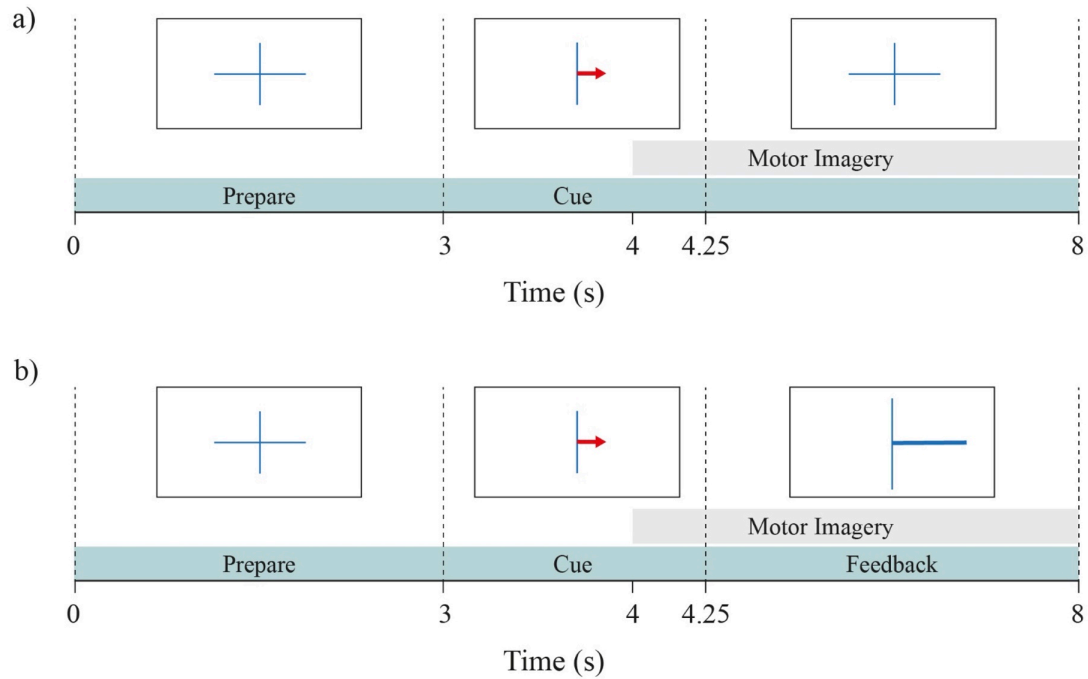
CNN Classification for Motor Imagery BCIs

180 **2.1.3 Motor Imagery Task**

181 Participants performed the MI task in four runs, each consisting of 20 right- and
182 twenty left-hand trials. The first run was a non-feedback run, followed by three runs
183 in which the subjects received feedback in form of a feedback bar on the computer
184 screen. The feedback bar presented the classification certainty as computed by the
185 g.tec BCI classifier, which relies on the CSP+LDA approach. The classifier was
186 calibrated for each subject based on the data of the latest run while the subject took a
187 break between the runs.

188 In total, participants performed 120 MI trials. Each MI trial took eight seconds. The
189 timeline of each trial is shown in [Figure 2](#). It started with a fixation cross that was
190 displayed in the center of the screen for three seconds. In the next 1.25 seconds, a red
191 arrow cued the direction of the trial; the subject had to imagine squeezing their left
192 hand if the arrow pointed to the left and their right hand if the arrow pointed to the
193 right, without tensing their muscles. During the last 3.75 seconds, the calibration run
194 showed the fixation cross again (see [Figure 2a](#)), while the feedback runs showed a
195 blue feedback-bar indicating the direction and certainty of the algorithms'
196 classification (see [Figure 2b](#)). Participants were instructed to stay focused on the
197 imagination of the movement even during the feedback and try to not get distracted by
198 it. The end of the trial was marked by a blank screen. The rest time between trials
199 varied randomly between 0.5 and 2.5 seconds.

CNN Classification for Motor Imagery BCIs



200

201 **FIGURE 2** | The time course of each trial in the BCI task. (a) shows the calibration
202 run and (b) the feedback runs. In all trials, participants saw a fixation cross and
203 thereafter an arrow pointing to either left or right, which indicated the corresponding
204 hand for the MI task in the trial. In feedback runs, the blue bar indicated the direction
205 and certainty of the classifier's prediction in order to feedback to the participants. The
206 grey area indicates the time course of the MI task.

207

208 **2.1.4 EEG Dataset**

209 The signals from three participants were not recorded in a satisfactory manner due to
210 technical issues during the experiment. Hence, only 54 participants were chosen from
211 the dataset for this study. An epoch of 4 seconds was selected from each trial. This
212 epoch, targeting the MI period, started at second 4 of the trial (1 second after cue
213 presentation) and ended at second 8 (5 seconds after cue presentation), which is in
214 line with the study of Marchesotti et al. (2016). The selected time segment is indicated
215 with the grey area in [Figure 2](#).

216

CNN Classification for Motor Imagery BCIs

217 **2.2 Machine Learning Model**

218 The ML approach consisted of preprocessing the signals, constructing CSP filters for
219 feature extraction and an LDA model for classification of the left vs. right classes.

220 CSP is a feature extraction technique that selects spatial filters from multi-channel
221 signals and then linearly transforms EEG data into a subspace with lower dimension
222 that maximizes the variance of one class while minimizing the variance of the other
223 class ([Khan et al., 2019](#); [Shen et al., 2017](#)). CSP algorithm is widely used in binary
224 MI-BCIs due to its computational simplicity and improving signal to noise ratio
225 ([Bashashati et al., 2015](#); [Guan et al., 2019](#)). The output of CSP can be used as input
226 for the LDA classifier in order to distinguish the classes of MI task.

227 LDA is a dimensionality reduction model that works on the concept of minimizing the
228 ratio of within-class scatter to between-class scatter while keeping the intrinsic details
229 of the data intact ([Shashibala & Gawali, 2016](#)). Hence, LDA creates a hyperplane in
230 the feature space based on evaluation of the training data to maximize the distance
231 between the two classes and minimize the variance of the same class ([Aydemir &
232 Kayikcioglu, 2013](#); [Hasan et al., 2015](#)). LDA is very popular for binary classification
233 of the MI task ([Yuksel & Olmez, 2015](#)).

234 **2.2.1 Architecture**

235 Before applying the ML model, the EEG signals recorded from the participants were
236 pre-processed and temporally filtered to remove artifacts. Data containing bad
237 impedance, error in recording, or excessive movement-related noise were removed (3
238 subjects, see 2.1.4). Then the EEG signals corresponding to the onset of MI task
239 (second 4 to 8, see Figure 2) were selected and taken into account ([Park & Chung,
240 2019](#)). Thereon, Filter Bank Common Spatial Pattern (FBCSP) was used to extract

CNN Classification for Motor Imagery BCIs

241 subject-specific frequency band of 7-30 Hz from the data through the implementation
242 of fifth order Butterworth ([Park & Chung, 2019](#); [Lotte & Guan, 2011](#)).

243 FBCSP was used because it is instrumental in discriminating the binary classification
244 of EEG measurements ([Ang et al., 2012](#); [Raza et al., 2015](#); [Park & Chung, 2019](#)). It
245 should be noted that CSP is highly dependent on the selection of frequency bands,
246 however there is no optimal solution to select the right filter bank ([Kumar et al.,](#)
247 [2017](#)). Using a filter bank before CSP helps to improve the accuracy level of the
248 model ([Yahya et al., 2019](#)). A wide range of 7-30 Hz is usually adopted for CSP when
249 used for MI classification ([Kumar et al., 2017](#)). Hence, the frequency bandwidth was
250 kept between 7-30 Hz covering the mu and beta bands that are required to analyze
251 Event-Related Desynchronization (ERD) and Event-Related Synchronization (ERS)
252 from the MI brain signals.

253 After the pre-processing and filtering steps, the 120 MI trials of each participant were
254 concatenated and randomized. CSP algorithm was performed on each participant's
255 data using the '*scikit*' package in Python ([Yuksel & Olmez, 2015](#)). CSP extracted the
256 spatially distributed information from the output of FBCSP by linearly transforming
257 the EEG measurements in order to define discriminative ERD/ERS features ([Ang et](#)
258 [al., 2012](#); [Park & Chung, 2019](#); [Raza et al., 2015](#)). Once feature extraction was
259 completed, '*scikit*' package was again used to implement the LDA classifier in order
260 to reduce the dimensionality of the sub-bands and to perform binary classification
261 ([Vidaurre et al., 2011](#)).

262

263 **2.3 Deep Learning Model**

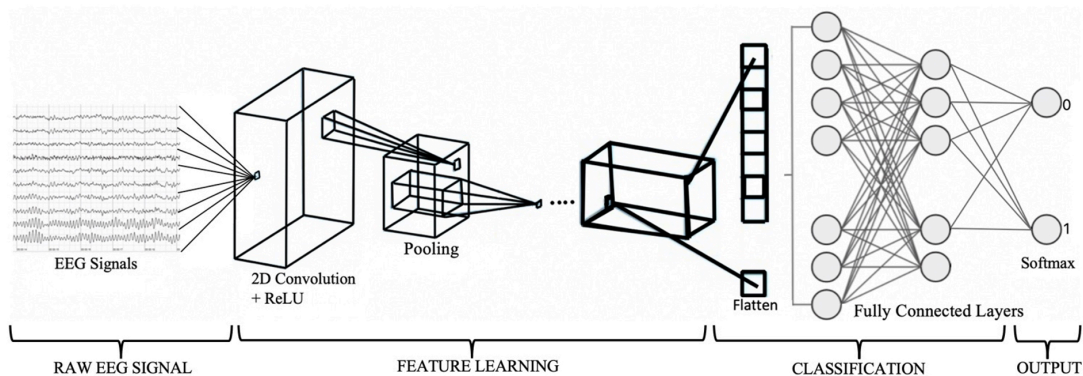
264 The DL model was constructed by feeding raw EEG signals directly into a CNN
265 model.

CNN Classification for Motor Imagery BCIs

266 CNN is a feed-forward Artificial Neural Network (ANN) model and has a sequence
267 of layers where every layer is the output of an activation using a differential function
268 ([Aggarwal & Chugh, 2019](#)). In a CNN, the inputs are assembled to different layers of
269 neurons, each representing a linear combination of the inputs ([Pérez-Zapata, 2019](#)).
270 The learning process involves modification of the parameters by adjusting weights
271 between different layers in order to achieve the desired output ([Roy et al., 2019](#)). The
272 learning continues until the training set reaches a steady state where the weights
273 become consistent and an optimal output is reached ([Roy et al., 2019](#)). During the
274 training phase of the CNN model, different layers can extract features at a different
275 level of abstraction ([Roy et al., 2019](#)). The initial layers learn local features from the
276 raw input, and the end layers learn global features ([Schirrmester et al., 2017](#)).

277 **2.3.1 Architecture**

278 A 2D CNN model was constructed using ‘*keras*’, a high-level neural networks API
279 written in Python (Keras, 2019). [Figure 3](#) shows the architecture of the proposed CNN
280 model.



281

282 **FIGURE 3** | CNN Architecture.

283

284 The first two components of the architecture are the number of convolution filters
285 used and the kernel size that specifies the height (columns) and width (rows) of the

CNN Classification for Motor Imagery BCIs

286 2D convolution window. These were set to 30 and 5×5 respectively. The dimensions
287 of the input shape applied were $(1 \times 4 \times 4)$. In order to compute a network's hidden
288 layers, activation functions should be implemented ([Goodfellow et al., 2016](#)). For this
289 task, Rectified Linear Function (ReLU) was used. ReLU conducts simple
290 mathematical operations, preserves characteristics that result in good generalization
291 and is less computationally expensive than other approaches. Moreover, ReLU has the
292 advantage of the speed and overcoming gradient leakage issue when compared with
293 other activation functions ([Pérez-Zapata, 2019](#)).

294 Max pooling was added to the model in order to downsample the input and refrain
295 from losing important data features. The size of 2×2 was used based on the works of
296 [Dharamsi et al. \(2017\)](#) and [Abbas and Khan \(2018\)](#). The output of max pooling was
297 flattened into a vector of input data by executing a flatten layer ([Goodfellow et al.,](#)
298 [2016](#)). Subsequently, three dense layers were added. The first two implemented a
299 linear function in which all inputs were connected to all outputs by a specific weight
300 ([Ullah et al., 2019](#)). The units of these were set to 256 and 128 and were activated by
301 ReLU functions. The final dense layer's units were fixed to 2 as this was the number
302 of class labels in the data. Finally, Softmax was applied to the last (output) layer as an
303 activation function, used for class classification tasks ([Goodfellow et al., 2016](#)).

304 **2.3.2 CNN Model Compilation**

305 The hyperparameters implemented in the 2D CNN model's compilation phase are the
306 loss function, the optimizer and the evaluation metric. Since the dataset has two target
307 labels (right and left), the loss function categorical cross-entropy was applied. The
308 optimizer 'Adam' was used because it is a widely used gradient-based optimization of
309 stochastic objective functions ([Kingma & Ba, 2014](#)). An essential parameter of
310 'Adam' is the learning rate, which regulates the modification of the model based on

CNN Classification for Motor Imagery BCIs

311 the error obtained from the updated weights ([Kingma & Ba, 2014](#)). For the task at
312 hand, the learning rate was set to its default value of 0.01. The evaluation metric was
313 set to accuracy to delineate how well the CNN model could classify left vs. right MI
314 EEGs. ([Goodfellow et al., 2016](#)).

315 ***2.3.3 CNN Model Fit***

316 During model fitting, a specified batch size and number of epochs need to be adopted
317 for backpropagation to take place ([Browniee, 2016](#)). The batch size greatly influences
318 the time to converge and the amount of overfitting ([Radiuk, 2018](#)); a big batch takes
319 into account many samples to calculate a gradient step and therefore might slow down
320 the model training ([Goodfellow et al., 2016](#)). On the other hand, small batch sizes can
321 supervise variation in the distribution. The batch size for the 2D CNN model was set
322 to 264.

323 An epoch in DL means that all the samples in the training set are traversing through
324 the model once ([Browniee, 2016](#)). This helps the network to see previous data for
325 readjusting the model parameters in order to reduce any biases. The neural network
326 updates the weights of the neuron during each epoch ([Torres, 2018](#)). However, there
327 is not any prescribed method to calculate how many epochs are required for a
328 particular model. Sharma ([2017](#)) stated that different values of epochs should be tried
329 until the learning curve of the model moves from underfitting to an optimum level and
330 until overfitting attributes start showing up, then the subsequent epoch size should be
331 deemed as the threshold for the model. Thus, as long as both training and test
332 accuracies are increasing at an equivalent rate, the training of the model should
333 continue ([TensorFlow, 2020](#)). Considering the arguments from Kingma and Ba ([2015](#))
334 and TensorFlow ([2020](#)), 500 epochs per subject was deemed to be the threshold for
335 the CNN model.

CNN Classification for Motor Imagery BCIs

336 **2.4 Evaluation**

337 For the CNN model, the data was split into 80% training and 20% test data. [Tang et](#)
338 [al. \(2017\)](#) used the same splitting variation for building their CNN model. Accuracy is
339 defined as the total amount of correct predictions that the model made including both
340 training and test accuracies ([Goodfellow et al., 2016](#)). Hereby, the mean accuracy
341 over all the subjects in training and test phase was calculated in order to compare the
342 performance of CSP+LDA and CNN models.

343 Additionally, we observed how the CNN model and CSP+LDA model performed
344 subject-wise by computing the difference of the two models' accuracy for each
345 subject. This was done to give greater validity to the findings as inter-subject
346 variability can affect the overall performance of a classifier ([Saha & Baumert, 2020](#)).

347 While accuracy is the overall evaluation measure of a model, it does not fully exhibit
348 its prediction capacity. Therefore, in addition to the overall prediction accuracy, we
349 extracted F-score metric for each class of 'left' or 'right' MI. F-score is the harmonic
350 mean of the precision and recall metrics and demonstrates the discriminant power of
351 the model for each existing class in the data. Previous research has shown that the
352 BCI user handedness plays a role in lateralization of ERD/ERS during the MI task
353 ([Zapala et al., 2020](#)). In our study, all subjects were right-handed, therefore it was
354 expected that the errors made by the model would be more for one MI class than the
355 other.

356

357 **3 Results**

358 The average score of the training and test accuracies across 54 subjects were taken
359 into consideration to report the performance level of the CNN and CSP+LDA models.
360 The CNN model reached an average training accuracy of 80.58% ($SD = 5.01$) and an

CNN Classification for Motor Imagery BCIs

361 average test accuracy of 69.42% ($SD = 4.97$), whereas the average training and test
362 accuracies for the CSP+LDA model were 52.54% ($SD = 5.12$) and 52.56% ($SD =$
363 2.08), respectively. [Table 1](#) gives a summary of these results.

364 **TABLE 1** | Comparison between training and test accuracies of CNN and CSP+LDA
365 models.

Model	Training Accuracy ($N=54$)		Test Accuracy ($N=54$)	
	Mean	SD	Mean	SD
CNN	80.58	5.01	69.42	4.97
CSP+LDA	52.54	5.12	52.56	2.08

366
367 The obtained accuracies for both CNN and CSP+LDA models were normally
368 distributed as evaluated with Shapiro-Wilk test (CNN: $W = 0.98$, $p = .66$; CSP+LDA:
369 $W = 0.97$, $p = .12$). Therefore, a pairwise t-test was employed to compare the test
370 accuracies obtained from the DL classification method to those of the ML approach
371 ($t(53) = 22.12$, $p < .001$). This indicated that the CNN classifier significantly
372 outperformed the CSP+LDA approach by 15.32 to 18.38% within the 95% confidence
373 interval.

374 [Table 2](#) contains the top ten accuracy rates observed in the subjects using the CNN
375 and the CSP+LDA model. As it can be seen in this table, the highest accuracy
376 achieved by the CNN model for a subject was 81.80%, whereas the CSP+LDA model
377 could only reach a highest accuracy rate of 57.17%. Also, although not included in
378 this table, it was observed that the lowest accuracy level obtained from the CNN

CNN Classification for Motor Imagery BCIs

379 model across all the subjects was 58.60%, which is still higher than the highest

380 accuracy rate obtained by the CSP+LDA model across all the subjects.

381 **TABLE 2** | Top ten highest classification accuracies achieved by the CNN model and

382 the CSP+LDA model.

CNN Model		CSP + LDA Model	
Participant ID	Accuracy %	Participant ID	Accuracy %
Subject 31	81.80	Subject 29	57.17
Subject 48	77.36	Subject 7	56.70
Subject 16	76.94	Subject 55	56.41
Subject 25	76.32	Subject 54	56.23
Subject 55	75.81	Subject 34	56.16
Subject 9	75.72	Subject 8	55.90
Subject 60	75.64	Subject 30	55.67
Subject 12	75.58	Subject 32	55.65
Subject 42	75.52	Subject 60	55.32
Subject 23	75.08	Subject 66	54.50

383

384 To obtain an estimation of the subject-wise performance difference between the two

385 models, the difference of the obtained accuracy from the CNN model and the

386 CSP+LDA model for each subject ($Accu_{CNN} - Accu_{CSP+LDA}$) was computed. This

387 subject-wise comparison revealed that the DL approach achieved a higher accuracy

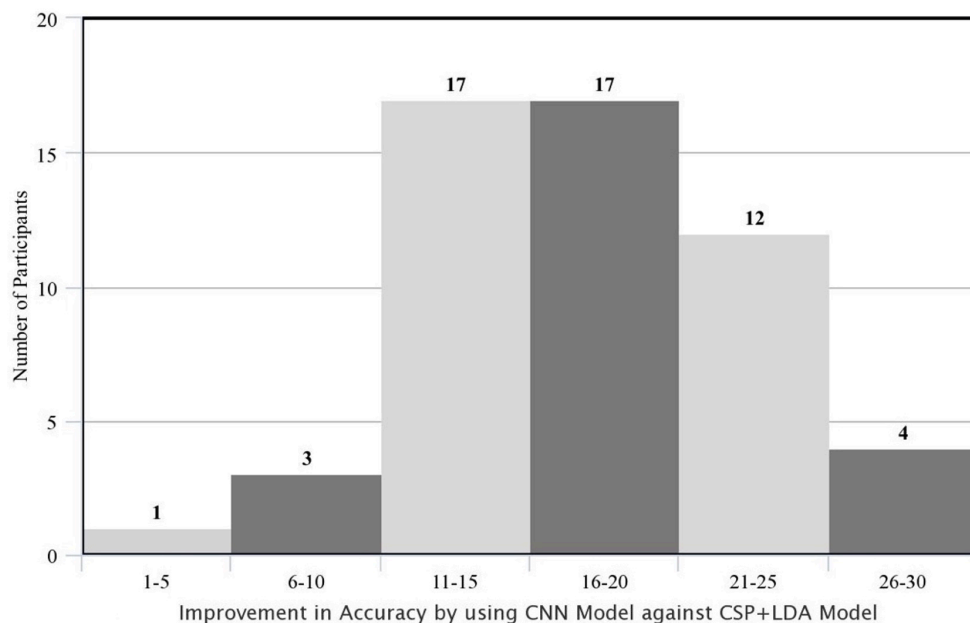
388 level for all subjects with a minimal difference of 2.37% and maximal difference of

389 28.28%. [Figure 4](#) illustrates the number of subjects for whom the CNN model showed

390 accuracy improvement in 6 bins of 1-5%, 6-10%, 11-15%, 16-20%, 21-25% and 26-

CNN Classification for Motor Imagery BCIs

391 30%. From this figure, it can be inferred that the CNN model outperformed the
392 CSP+LDA model by more than 11% accuracy for 92.59% of the participants.
393 Therefore, it can be concluded that CNN was able to extract intrinsic features from
394 the EEG signals and thereon, performed classification with higher accuracy level.

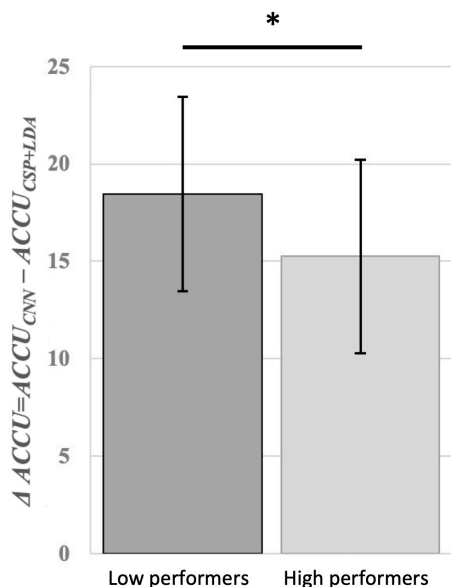


395
396 **FIGURE 4** | Improvement in the accuracy rate of the subjects using CNN model
397 against CSP+LDA in percent points (i.e., absolute difference between the two
398 accuracies; $\text{AccuCNN} - \text{AccuCSP+LDA}$).

399
400 Further exploration was done to investigate whether the improvement achieved by the
401 CNN model was different across BCI users based on their initial MI skill.
402 Traditionally, users that cannot produce desired ERD/ERS patterns to be recognized
403 by a MI-BCI classifier are defined as low aptitude users or BCI inefficient
404 ([Thompson, 2019](#)). Therefore, based on classification accuracy rates obtained from
405 the CSP+LDA model, subjects were divided into two groups of Low Performers and
406 High Performers. The split was made based on the accuracy median ($\text{Med} = 52.14\%$),
407 resulting in 27 subjects per group. For each group, the improvement of classification

CNN Classification for Motor Imagery BCIs

408 performance from the CSP+LDA model to the CNN model was obtained per subject
409 by subtracting the model accuracies ($\Delta Accu = Accu_{CNN} - Accu_{CSP+LDA}$).
410 [Figure 5](#) shows the mean accuracy improvement ($\Delta Accu$) for each group. On average,
411 the CNN model increased the accuracy rate of the Low Performers by 18.46% ($SD =$
412 4.98%) and the High Performers by 15.25% ($SD = 5.81\%$). The obtained $\Delta Accu$
413 values for both Low Performer and High Performer groups were normally distributed
414 as evaluated with Shapiro-Wilk test (Low Performers: $W = 0.96, p = .47$; High
415 Performers: $W = 0.98, p = .84$). Therefore, an independent t-test was employed to
416 compare them, revealing a significantly higher improvement of classification
417 performance by the CNN model for Low Performers ($t(26) = 2.18, p < .05$). This
418 result supports the notion that the CNN model can better capture intrinsic oscillation
419 patterns associated with the MI task in inefficient BCI users, whose modulation of
420 SMR cannot be successfully recognized by the CSP+LDA model.



421

422 **FIGURE 5** | Mean difference between accuracies of CNN and CSP+LDA models
423 ($Accu_{CNN} - Accu_{CSP+LDA}$) for Low Performer and High Performer groups. Low
424 Performers showed significantly higher improvement in MI-BCI accuracy after using
425 a CNN classifier.

CNN Classification for Motor Imagery BCIs

426 Finally, F-Score was calculated for each class in order to measure the predictive
 427 power of the classifiers with respect to the ‘*left*’ or ‘*right*’ MI movements. [Table 3](#)
 428 summarizes the average and SD of F-Scores across all subjects obtained by the CNN
 429 and CSP+LDA models in regard to each MI class. As can be seen in this table, the
 430 CNN model achieved higher F-Score values for both ‘*left*’ and ‘*right*’ hand prediction
 431 compared to the CSP+LDA model. A pairwise t-test comparing the F-Scores of the
 432 two models found a significant difference for both ‘*left*’ MI movements ($t(53) =$
 433 $18.28, p < .05$) as well as ‘*right*’ MI movements ($t(53) = 19.47, p < .05$) favoring
 434 CNN as a classifier beyond CSP+LDA approach.

435 **TABLE 3** | Average F-score obtained by the CNN and CSP+LDA models for each
 436 MI class.

Evaluation Metric	CNN Model				CSP + LDA Model			
	Left Hand <i>(N=54)</i>		Right Hand <i>(N=54)</i>		Left Hand <i>(N=54)</i>		Right Hand <i>(N=54)</i>	
	Mean	SD	Mean	SD	Mean	SD	Mean	SD
F-Score (%)	69.07	5.35	68.59	5.23	52.93	3.67	51.83	3.56

437

438

439 **4 Discussion**

440 In order for a BCI system to operate optimally for all users, it is crucial to devise a
 441 classification model that can learn from each individual’s brain signals and recognize
 442 task-related patterns with high accuracy. In this research, a CNN model was
 443 developed on a large EEG dataset from 54 subjects who conducted MI task during a
 444 BCI interaction. The main goal of this study was to validate that a DL approach
 445 employing raw EEG signals could outperform the state-of-the-art MI-BCIs, which

CNN Classification for Motor Imagery BCIs

446 often employ ML approach including CSP algorithm for feature extraction and LDA
447 model for classification. Our results supported this hypothesis; the CNN model
448 displayed significantly higher classification accuracy for the MI task as compared to
449 the CSP+LDA approach for all users, but especially benefited low aptitude users by
450 increasing their BCI performance significantly more than high aptitude users. Our
451 results put forward the design of future BCI classifiers that facilitate better interaction
452 between the user and the BCI system.

453 Until now, an in-depth analysis of a CNN model in which a large and novel dataset of
454 raw EEG signals were directly fed to the model for classification of the MI task was
455 still missing. Previous studies mainly focused on comparing different ML and DL
456 models on already existing datasets. For instance, [Sakhavi et al. \(2015\)](#) employed the
457 BCI competition IV (Dataset 2b) for multi-class classification of MI task. Their CNN
458 model achieved accuracy level of 69.56%, whereas their Support Vector Machine
459 (SVM) model, Multi Layer Perceptron (MLP) model and CNN+MLP model achieved
460 accuracy level of 67.01%, 65.78% and 70.60%, respectively. Likewise, [Li et al.](#)
461 [\(2020\)](#) used BCI competition IV (Dataset 2b) but the authors combined different
462 feature extraction techniques with their ML and DL models to conduct comparison
463 between these models. [Li et al. \(2020\)](#) showed that a combination of Continuous
464 Wavelet Transform (CWT) with Simplified Convolutional Neural Network (SCNN)
465 model achieved an average accuracy of 83%, which was 7.22%, 9.62%, 10.93%,
466 7.49%, 6.94%, 5.58% and 5.05 % higher than CNN+Stacked AutoEncoders (SAE),
467 CSP, Adaptive Common Spatial Pattern (ACSP), Deep Belief Network (DBN),
468 CSP+SCNN, Fourier Transform (FFT)+SCNN and Short Time Fourier transform
469 (STFT)+SCNN, respectively. In another study by [Gao et al. \(2018\)](#), CSP was used for
470 feature extraction and the CNN model was combined with Sparse Representation-

CNN Classification for Motor Imagery BCIs

471 based Classification (SRC) algorithm for binary classification of the MI task. The
472 dataset adopted by [Gao et al. \(2018\)](#) was BCI competition III (Dataset IVa). Here the
473 authors showed that their SRC+CNN model achieved mean accuracy of 80% ([Gao et](#)
474 [al., 2018](#)).

475 Although previous studies provided promising results with a DL approach, the
476 employed dataset by [Sakhavi et al. \(2015\)](#) and [Li et al. \(2020\)](#) only included nine
477 subjects and the dataset used by Gao et al. (2018) only had five subjects. These
478 datasets do not sufficiently represent the large inter-subject variability that exist
479 among users ([Leeuwis & Alimardani, 2020](#)), which could affect the performance of
480 the classifier. Different BCI users have a different state of mind, and hence different
481 spatial, spectral and temporal patterns in their EEG signals ([Ahn & Jun, 2015](#)). Such
482 variations can be due to the difference in the concentration levels of the participants
483 while performing the MI task or baseline cognitive and psychological abilities
484 ([Leeuwis et al., 2021](#)). Thus, it is necessary to perform BCI studies over a diverse and
485 large pool of subjects in order to establish the broad generalizability of the findings.

486 In comparison to previous studies that only employed datasets with limited number of
487 participants and trials, this study collected MI EEG signals from 54 participants in
488 three runs (120 trials) and built a 2D CNN model on our dataset. The large number of
489 subjects in this dataset enabled us to statistically compare the subject-wise
490 performance achieved by the CNN model as compared to the conventional ML
491 approach. The results showed that the CNN model achieved an average of 69.42%
492 accuracy across all subjects, which is similar to the CNN accuracy rate achieved by
493 [Sakhavi et al. \(2015\)](#) who used feature engineering techniques to enhance the
494 performance of their CNN model. The accuracy level achieved by this study might
495 initially seem insufficient when compared to [Gao et al. \(2018\)](#) and [Li et al. \(2020\)](#),

CNN Classification for Motor Imagery BCIs

496 however, this difference can be explained by various pre-processing and feature
497 engineering techniques that were employed by these two studies. Unlike past
498 research, this study focused on evaluating the performance of CNN model without
499 implementing any fine-tuning techniques and by directly feeding raw data into the
500 model. The motive for this approach was to show the efficacy of deep learning
501 models in exploiting information from raw data without any need for feature
502 extraction. This makes deep learning models computationally more effective by
503 eliminating the costly steps of pre-processing and feature extraction. Additionally,
504 such neural networks can handle noise in EEG signals better than ML models and
505 thus can provide a more robust performance in real-time BCI applications.

506 The low performance obtained in the ML approach has to be compared to the online
507 classification accuracies presented in [Leeuwis et al. \(2021\)](#), where the average
508 classification accuracy was 74.17%. This could be explained by different
509 architectures: The online classification of [Leeuwis et al. \(2021\)](#) was conducted by
510 g.BSanalyze software (g.tec Medical Engineering, Austria) . In this model, baseline
511 non-feedback data is provided to the model to calibrate the classifier for each subject
512 before the actual classification runs. In addition, the lack of removal of bad trials in
513 our ML approach may explain a difference in the acquired classification accuracies.

514 Also, in [Leeuwis et al. \(2021\)](#) subjects were trained upon online classification,
515 optimizing performance for that specific processing pipeline. Therefore, to make a
516 fair comparison with our DL model, we employed a ML approach using offline
517 classification with no prior training and calibration of the system.

518 With recent release of large scale EEG datasets (e.g. [Cho et al., 2017](#); [Lee et al. 2019](#)),
519 there have been more attempts on employing DL models on signals from large
520 number of participants (e.g., [Stieger et al., 2020](#); [Zhang et al., 2021](#); [Ko et al., 2020](#);

CNN Classification for Motor Imagery BCIs

521 [Mane et al., 2020](#)), showing the relevance and timeliness of this study in the BCI
522 field. Although these studies report the same conclusion for superiority of the DL
523 approach in MI-BCI classification, their methodology and approach in building the
524 DL model is different from our study. For instance, [Stieger et al. \(2020\)](#) trained a
525 CNN model with high density EEG (64 channel) to classify a 4-class MI task. [Mane](#)
526 [et al. \(2020\)](#) and [Ko et al. \(2020\)](#) focused on feature representations in the model;
527 [Mane et al. \(2020\)](#) employed Filter-Bank CNN to decompose data into multiple
528 frequency bands and extract spatially discriminative patterns in each band, and [Ko et](#)
529 [al. \(2020\)](#) applied a Multi-Scale Neural Network to exploit spatio-spectral-temporal
530 features for all BCI paradigms. [Zhang et al. \(2021\)](#) focused on transfer learning and
531 employed a CNN model to develop a subject-independent classifier. Therefore, while
532 our study pursues a similar goal, it dissociates itself from past research by conducting
533 a statistically supported subject-wise comparison between the DL and ML approaches
534 and also providing evidence for suitability of the DL approach for inefficient BCI
535 users.

536 As mentioned before, difference between our study and for example [Sakhavi et al.](#)
537 [\(2015\)](#), [Gao et al. \(2018\)](#) and [Li et al. \(2020\)](#) is the employment of pre-processing and
538 feature extraction techniques before applying a DL approach. The only previous study
539 that concentrated on building a CNN model for classification of binary class MI task
540 without implementing any feature engineering technique was conducted by [Tang et al.](#)
541 [\(2017\)](#), who achieved 86% mean accuracy for their CNN model. However, they
542 recorded EEG signals from 28 electrodes (as compared to 16 electrodes in this study)
543 and their subject size was only two, which does not provide a suitable representation
544 of the general MI-BCI users. Additionally, [Tang et al. \(2017\)](#) applied 8–30 Hz
545 bandpass filter on the raw data before passing them to the model and the subjects in

CNN Classification for Motor Imagery BCIs

546 their study did not receive any feedback during the MI task, which is an important
547 factor in MI learning and online operation of the BCI systems ([Alimardani et al.,](#)
548 [2016](#)). This makes it difficult to interpret the outcome of [Tang et al. \(2017\)](#) and can
549 perhaps explain the higher accuracy that was achieved by them. In this study, we
550 recruited 54 participants including MI-BCI inefficients ([Leeuwis & Alimardani, 2020](#))
551 and ensured that the participants were learning during the experiment through practice
552 trials and feedback provided by the BCI system.

553 An important finding of this study was that the CNN model outperformed the
554 CSP+LDA model for all of the subjects, achieving 11-30% accuracy improvement for
555 92.59% of the subjects. Hence, deducing from the better performance of the DL
556 model compared to ML approach and also from previous studies ([Sakhavi et al.,](#)
557 [2015](#); [Gao et al., 2018](#); [Li et al., 2020](#); [Tang et al., 2017](#); [Stieger et al., 2020](#); [Zhang et](#)
558 [al., 2021](#); [Ko et al., 2020](#); [Mane et al., 2020](#)), it can be concluded that regardless of the
559 users' ability to generate MI-specific sensorimotor oscillations, CNN models are more
560 effective in extracting intrinsic features from EEG signals and thereon, can perform
561 MI classification with higher accuracy level. This study also revealed that the CNN
562 model was able to capture better understanding of the MI brain patterns in inefficient
563 users than the CSP+LDA model. CNN significantly improved the classification
564 accuracy for those users whose performance was lower when the conventional
565 CSP+LDA model was adopted.

566 BCI inefficiency has long been seen as a human factor problem in the literature. Only
567 recently, [Stieger et al. \(2020\)](#) suggested that DL approaches might increase accuracies
568 for low aptitude performers, thereby enabling some of them to reach performance
569 above the threshold of 70% accuracy. Our study supports their finding by showing
570 that indeed; the DL approach could significantly improve the classification

CNN Classification for Motor Imagery BCIs

571 performance of low performers, supporting the arguments by [Thompson \(2019\)](#), who
572 states that poor performance of training should not be always blamed on the user.
573 Hereby, this study shows that designing an effective classifier using a DL approach
574 could be more reliable in developing robust MI-BCI applications and this also
575 overcomes the issues with BCI inefficiency.
576 Yet another advantage of the DL approach is that it allows automatic discovery of
577 discriminative features in raw data. Therefore, it is reasonable to consider recording
578 and inclusion of more EEG signals from other brain regions for the model training.
579 [Stieger et al. \(2020\)](#) showed that motor imagery processes might be extended beyond
580 the sensorimotor cortex and mu suppression patterns, indicating that the application of
581 deep learning might be beneficial in extracting such brain activity patterns for
582 inefficient users. Future research can extend our findings by employing a full-scalp
583 recording and showing how this can impact the performance of the CNN model
584 across subjects and thereby future design of more individual-tailored classifiers for all
585 users, especially inefficient users.
586 The BCI performance is a product of the interplay between the BCI system and the
587 user ([Alimardani et al., 2014](#)); therefore, the importance of user training and the
588 ‘*human in the loop*’ cannot be overlooked. Motivation and feedback play an important
589 role in user’s learning of the MI task ([Roc et al., 2020](#), [Alimardani et al., 2018](#)).
590 Hence, interaction with a MI-BCI should be established on an engaging platform
591 where the users feel engaged and enjoy the process during experimentation ([Roc et](#)
592 [al., 2020](#); [Femke et al., 2010](#)). Additionally, detailed instructions on how to perform
593 the mental task of MI should be provided to the users to give them a clear cognitive
594 strategy during BCI training ([Roc et al., 2020](#)). This helps to offset the cognitive load
595 on participants and results in stable brain signals, which in turn contributes towards

CNN Classification for Motor Imagery BCIs

596 developing an efficient BCI system ([Roc et al., 2020](#)). This study employed a classic
597 screen-based feedback bar to provide feedback to the user during data collection. Past
598 studies have shown that embodied feedback in form of virtual or robotic hands can
599 improve interaction between the user and the BCI system ([Skola & Liarokapis, 2018](#);
600 [Alimardani et al., 2016](#)). Future studies should attempt to replicate the results of this
601 study with a more engaging and realistic feedback that could lead to generation of
602 more distinguished brain patterns by the user at the data collection stage.

603 Although this study presents evidence that a DL approach outperforms a ML model
604 for subject-specific classification of the MI task, the question remains whether the
605 proposed CNN model will be able to perform equally well on new subjects who might
606 have different EEG signals. A general challenge in the development and application
607 of MI-BCI systems is their long calibration time ([Singh et al., 2019](#)). In order to
608 reduce the calibration time or completely eliminate it, past research has proposed
609 transfer learning in which common information across subjects or sessions is mined
610 and used for training of the classifier to improve the prediction for a new target
611 subject ([Azab et al., 2019](#)). However, most transfer learning methodologies focus on
612 extracting features and adapting them from the source subject(s) to the target subject,
613 whereas in DL models with an end-to-end decoding, the neural network itself should
614 be able to do this with little data pre-processing ([Zhang et al., 2021](#)). Thus, it becomes
615 important to expand this research in the future with transfer learning methods and
616 evaluate the performance of the proposed CNN model on new targets.

617 In this study, classification was performed offline. This is not suitable for continuous
618 BCI control where the classifier is constantly updated ([Wolpaw & McFarland, 2004](#)),
619 because fluidly controlling an external device is not equal to outputting one command
620 at the end of a trial ([Edelman et al., 2019](#)). [Stieger et al. \(2020\)](#) simulated continuous

CNN Classification for Motor Imagery BCIs

621 control by providing feedback based on the estimated class output of their CNN every
622 40 milliseconds and showed that CNN applied on all 64 electrodes made decisions
623 earlier with the threshold degree of confidence and could therefore be applied to make
624 faster decisions in continuous control compared to CNN trained on only motor area
625 electrodes. Their proposal suggests that CNN is applicable for continuous control.
626 Therefore, the accuracy of our classifier providing online continuous feedback should
627 be examined in future research.

628 In sum, this study aimed to show the potential of DL for MI-EEG classification as
629 opposed to the state-of-the-art ML classifiers. Our results show that compared to the
630 conventional CSP+LDA model, the CNN model, which was trained and tested on raw
631 EEG signals, could achieve significantly higher classification performance for all
632 users, but especially for inefficient users. Applying DL to BCI applications is a
633 burgeoning field, which requires large dataset for development and validation. This
634 study dissociates itself from previous reports by employing a large dataset of 54
635 subjects and thus sufficiently reflecting the inter-subject variability among BCI users.
636 One of the main advantages of using DL classifier is to eliminate the pre-processing
637 and feature extraction stages used to build an ML classifier. Raw data collected from
638 EEG can directly be fed into a DL classifier. Future studies should be conducted by
639 deploying the proposed CNN model on new subjects to evaluate the performance of
640 the model and to examine whether the same model can be employed for subject-
641 independent classifiers.

642

643 **5 Conclusion**

644 In this research, we evaluated the benefits of DL in improving the performance of
645 motor imagery BCIs. We extracted the performance of a CNN model trained on raw

CNN Classification for Motor Imagery BCIs

646 EEG signals from 54 subjects and statistically compared it to that of CSP+LDA,
647 which is a popular ML classifier for binary classification of the MI task. The results
648 revealed that the CNN model significantly outperformed the traditional CSP+LDA
649 classifier by increasing classification accuracy for all 54 subjects in this study.
650 Moreover, it was shown that the CNN model benefited the inefficient BCI users
651 significantly more than high performers. Thus, we conclude that DL classifiers show
652 promise for future MI-BCI applications for all users as opposed to current state-of-art
653 ML-based BCI systems, which demand extensive effort in pre-processing and feature
654 extraction and yet are impractical for some users. Future studies should further
655 investigate the robustness of the proposed CNN model in real-time MI-BCI
656 applications

657

658 **6 Acknowledgements**

659 Authors would like to thank Alissa Paas for her assistance in collecting the data.

660

661 **7 Conflict of interest**

662 The authors declare no conflict of interest. One of the authors (NL) has a secondary
663 affiliation with a commercial company, Unravel Research, however this does not alter
664 our adherence to PLOS ONE policies on sharing data and materials as the data is
665 owned by Tilburg University.

666

667 **8 Funding statement**

668 This research was made possible in part through funding from the municipality of
669 Tilburg, Netherlands, on the MindLabs initiative. Unravel research provided support
670 in the form of salary for the second author (NL), but did not have any additional role

CNN Classification for Motor Imagery BCIs

671 in the study design, data collection and analysis, decision to publish, or preparation of
672 the manuscript.

673

674 **9 References**

- 675 Abbas W, Khan NA. DeepMI: deep learning for multiclass motor imagery
676 classification. In 2018 40th Annual International Conference of the IEEE
677 Engineering in Medicine and Biology Society (EMBC) 2018 Jul 18 (pp. 219-
678 222). IEEE. doi: [10.1109/EMBC.2018.8512271](https://doi.org/10.1109/EMBC.2018.8512271)
- 679 Aggarwal S, Chugh N. Signal processing techniques for motor imagery brain
680 computer interface: A review. *Array*. 2019 Jan 1;1:100003. doi:
681 [10.1016/j.array.2019.100003](https://doi.org/10.1016/j.array.2019.100003)
- 682 Ahn M, Jun SC. Performance variation in motor imagery brain-computer interface: a
683 brief review. *Journal of Neuroscience Methods*. 2015 Mar 30;243:103-10. doi:
684 [10.1016/j.jneumeth.2015.01.033](https://doi.org/10.1016/j.jneumeth.2015.01.033)
- 685 Al-Ani T, Trad D, Somerset VS. Signal processing and classification approaches for
686 brain-computer interface. *Intelligent and Biosensors*. 2010 Jan 1:25-66. doi:
687 [10.5772/7032](https://doi.org/10.5772/7032)
- 688 Albawi S, Bayat O, Al-Azawi S, Ucan ON. Social touch gesture recognition using
689 convolutional neural network. *Computational Intelligence and Neuroscience*.
690 2018 Oct 8;2018. doi: [10.1155/2018/6973103](https://doi.org/10.1155/2018/6973103)
- 691 Alimardani M, Nishio S, Ishiguro H. Effect of biased feedback on motor imagery
692 learning in BCI-teleoperation system. *Frontiers in Systems Neuroscience*.
693 2014 Apr 9;8:52. doi: [10.3389/fnsys.2014.00052](https://doi.org/10.3389/fnsys.2014.00052)

CNN Classification for Motor Imagery BCIs

- 694 Alimardani M, Nishio S, Ishiguro H. The importance of visual feedback design in
695 BCIs; from embodiment to motor imagery learning. PloS one. 2016 Sep
696 6;11(9):e0161945. doi: [10.1371/journal.pone.0161945](https://doi.org/10.1371/journal.pone.0161945)
- 697 Alimardani M, Nishio S, Ishiguro H. Brain-computer interface and motor imagery
698 training: The role of visual feedback and embodiment. Evolving BCI Therapy-
699 Engaging Brain State Dynamics. 2018 Oct 17;2:64. doi:
700 [10.5772/intechopen.78695](https://doi.org/10.5772/intechopen.78695)
- 701 Allison BZ, Neuper C. Could anyone use a BCI?. In Brain-computer interfaces 2010
702 (pp. 35-54). Springer, London. doi: [10.1007/978-1-84996-272-8_3](https://doi.org/10.1007/978-1-84996-272-8_3)
- 703 Alom MZ, Taha TM, Yakopcic C, Westberg S, Sidike P, Nasrin MS, Van Esesn BC,
704 Awwal AA, Asari VK. The history began from alexnet: A comprehensive
705 survey on deep learning approaches. arXiv preprint arXiv:1803.01164. 2018
706 Mar 3.
- 707 AlZoubi O, Koprinska I, Calvo RA. Classification of brain-computer interface data.
708 In Proceedings of the 7th Australasian Data Mining Conference-Volume 87
709 2008 Nov 27 (pp. 123-131).
- 710 Ang KK, Chin ZY, Wang C, Guan C, Zhang H. Filter bank common spatial pattern
711 algorithm on BCI competition IV datasets 2a and 2b. Frontiers in
712 Neuroscience. 2012 Mar 29;6:39. doi: [10.3389/fnins.2012.00039](https://doi.org/10.3389/fnins.2012.00039)
- 713 Avanzini P, Fabbri-Destro M, Dalla Volta R, Daprati E, Rizzolatti G, Cantalupo G.
714 The dynamics of sensorimotor cortical oscillations during the observation of
715 hand movements: an EEG study. PLoS One. 2012 May 18;7(5):e37534. doi:
716 [10.1371/journal.pone.0037534](https://doi.org/10.1371/journal.pone.0037534)
- 717 Aydemir O, Kayikcioglu T. Comparing common machine learning classifiers in low-
718 dimensional feature vectors for brain computer interface applications.

CNN Classification for Motor Imagery BCIs

- 719 International Journal of Innovative Computing, Information and Control. 2013
720 Mar;9(3):1145-57.
- 721 Azab AM, Mihaylova L, Ang KK, Arvaneh M. Weighted transfer learning for
722 improving motor imagery-based brain–computer interface. IEEE Transactions
723 on Neural Systems and Rehabilitation Engineering. 2019 Jun 17;27(7):1352-9.
724 doi: [10.1109/TNSRE.2019.2923315](https://doi.org/10.1109/TNSRE.2019.2923315)
- 725 Barros ES, Neto N. Classification Procedure for Motor Imagery EEG Data.
726 In International Conference on Augmented Cognition 2018 Jul 15 (pp. 201-
727 211). Springer, Cham. doi: [10.1007/978-3-319-91470-1_17](https://doi.org/10.1007/978-3-319-91470-1_17)
- 728 Bashashati H, Ward RK, Birch GE, Bashashati A. Comparing different classifiers in
729 sensory motor brain computer interfaces. PloS one. 2015 Jun
730 19;10(6):e0129435. doi: [10.1371/journal.pone.0129435](https://doi.org/10.1371/journal.pone.0129435)
- 731 Bharne PP, Kapgate DA. Review of Classification Techniques in Brain Computer
732 Interface. International Journal of Computer Sciences and Engineering.
733 2014;2:68-72.
- 734 Browniee, J. 5 Step Life-Cycle for Neural Network Models in Keras. Machine
735 Learning Mastery. 2016. Retrieved from [https://machinelearningmastery.com:
736 https://machinelearningmastery.com/ 5-step-life-cycle-neural-network-models
737 keras/](https://machinelearningmastery.com/https://machinelearningmastery.com/5-step-life-cycle-neural-network-models-keras/). [Accessed May 1, 2020]
- 738 Cho H, Ahn M, Kwon M, Jun SC. A step-by-step tutorial for a motor imagery–based
739 BCI. In Brain–Computer Interfaces Handbook 2018 Jan 9 (pp. 445-460). CRC
740 Press.
- 741 Cho H, Ahn M, Ahn S, Kwon M, Jun SC. EEG datasets for motor imagery brain–
742 computer interface. GigaScience. 2017 Jul;6(7):gix034. doi:
743 [10.1093/gigascience/gix034](https://doi.org/10.1093/gigascience/gix034)

CNN Classification for Motor Imagery BCIs

- 744 Craik A, He Y, Contreras-Vidal JL. Deep learning for electroencephalogram (EEG)
745 classification tasks: a review. *Journal of Neural Engineering*. 2019 Apr
746 9;16(3):031001. doi: [10.1088/1741-2552/ab0ab5](https://doi.org/10.1088/1741-2552/ab0ab5)
- 747 Dai M, Zheng D, Na R, Wang S, Zhang S. EEG classification of motor imagery using
748 a novel deep learning framework. *Sensors*. 2019 Jan;19(3):551. doi:
749 [10.3390/s19030551](https://doi.org/10.3390/s19030551)
- 750 Dharamsi T, Das P, Pedapati T, Bramble G, Muthusamy V, Samulowitz H, Varshney
751 KR, Rajamanickam Y, Thomas J, Dauwels J. Neurology-as-a-Service for the
752 Developing World. arXiv preprint arXiv:1711.06195. 2017 Nov 16.
- 753 Edelman BJ, Meng J, Suma D, Zurn C, Nagarajan E, Baxter BS, Cline CC, He B.
754 Noninvasive neuroimaging enhances continuous neural tracking for robotic
755 device control. *Science robotics*. 2019 Jun 19;4(31). doi:
756 [10.1126/scirobotics.aaw6844](https://doi.org/10.1126/scirobotics.aaw6844)
- 757 Nijboer F, Birbaumer N, Kubler A. The influence of psychological state and
758 motivation on brain–computer interface performance in patients with
759 amyotrophic lateral sclerosis—a longitudinal study. *Frontiers in Neuroscience*.
760 2010 Jul 21;4:55. doi: [10.3389/fnins.2010.00055](https://doi.org/10.3389/fnins.2010.00055)
- 761 Gao G, Shang L, Xiong K, Fang J, Zhang C, Gu X. EEG classification based on
762 sparse representation and deep learning. *NeuroQuantology*. 2018;16(6). doi:
763 [10.14704/nq.2018.16.6.1666](https://doi.org/10.14704/nq.2018.16.6.1666)
- 764 Goodfellow, I., Bengio, Y., & Courville, A. *Deep Learning* (Vol. URL
765 (<http://www.deeplearningbook.org>)). MIT Press. 2016. Retrieved from
766 <http://www.deeplearningbook.org>. [Accessed April 20, 2019]

CNN Classification for Motor Imagery BCIs

- 767 Guan S, Zhao K, Yang S. Motor imagery EEG classification based on decision tree
768 framework and Riemannian geometry. Computational Intelligence and
769 Neuroscience. 2019 Jan 21;2019. doi: [10.1155/2019/5627156](https://doi.org/10.1155/2019/5627156)
- 770 Hasan MR, Ibrahimy MI, Motakabber SM, Shahid S. Classification of multichannel
771 EEG signal by linear discriminant analysis. In Progress in Systems
772 Engineering 2015 (pp. 279-282). Springer, Cham.
- 773 Hsu WY. EEG-based motor imagery classification using neuro-fuzzy prediction and
774 wavelet fractal features. Journal of Neuroscience Methods. 2010 Jun
775 15;189(2):295-302. doi: [10.1016/j.jneumeth.2010.03.030](https://doi.org/10.1016/j.jneumeth.2010.03.030)
- 776 Keras. Convolutional Layers. Keras Documentation. 2019. Retrieved from
777 <https://keras.io/layers/convolutional/>. [Accessed March 20, 2019].
- 778 Khan J, Bhatti MH, Khan UG, Iqbal R. Multiclass EEG motor-imagery classification
779 with sub-band common spatial patterns. EURASIP Journal on Wireless
780 Communications and Networking. 2019 Dec;2019(1):1-9. doi:
781 [10.1186/s13638-019-1497-y](https://doi.org/10.1186/s13638-019-1497-y)
- 782 Kingma DP, Ba J. Adam: A method for stochastic optimization. arXiv preprint
783 arXiv:1412.6980. 2014 Dec 22.
- 784 Ko W, Jeon E, Jeong S, Suk HI. Multi-Scale Neural Network for EEG Representation
785 Learning in BCI. IEEE Computational Intelligence Magazine. 2021 Apr
786 13;16(2):31-45.
- 787 Kosmyna N, Lécuyer A. A conceptual space for EEG-based brain-computer
788 interfaces. PloS one. 2019 Jan 3;14(1):e0210145. doi:
789 [10.1371/journal.pone.0210145](https://doi.org/10.1371/journal.pone.0210145)
- 790 Kumar S, Sharma A, Tsunoda T. An improved discriminative filter bank selection
791 approach for motor imagery EEG signal classification using mutual

CNN Classification for Motor Imagery BCIs

- 792 information. BMC bioinformatics. 2017 Dec;18(16):125-37. doi:
793 [10.1186/s12859-017-1964-6](https://doi.org/10.1186/s12859-017-1964-6)
- 794 Kwon OY, Lee MH, Guan C, Lee SW. Subject-independent brain–computer
795 interfaces based on deep convolutional neural networks. IEEE Transactions on
796 Neural Networks and Learning Systems. 2019 Nov 13;31(10):3839-52. doi:
797 [10.1109/TNNLS.2019.2946869](https://doi.org/10.1109/TNNLS.2019.2946869)
- 798 Lebedev MA, Nicolelis MA. Brain-machine interfaces: From basic science to
799 neuroprostheses and neurorehabilitation. Physiological Reviews. 2017
800 Apr;97(2):767-837. doi: [10.1152/physrev.00027.2016](https://doi.org/10.1152/physrev.00027.2016)
- 801 Lee MH, Kwon OY, Kim YJ, Kim HK, Lee YE, Williamson J, Fazli S, Lee SW. EEG
802 dataset and OpenBMI toolbox for three BCI paradigms: an investigation into
803 BCI illiteracy. GigaScience. 2019 May;8(5):giz002. doi:
804 [10.1093/gigascience/giz002](https://doi.org/10.1093/gigascience/giz002)
- 805 Leeuwis N, Alimardani M. High Aptitude Motor-Imagery BCI Users Have Better
806 Visuospatial Memory. In 2020 IEEE International Conference on Systems,
807 Man, and Cybernetics (SMC) 2020 Oct 11 (pp. 1518-1523). IEEE.
- 808 Leeuwis N, Paas A, Alimardani M. Vividness of Visual Imagery and Personality
809 Impact Motor-Imagery Brain Computer Interfaces. Frontiers in Human
810 Neuroscience. 2021;15. doi: [10.3389/fnhum.2021.634748](https://doi.org/10.3389/fnhum.2021.634748)
- 811 Li F, He F, Wang F, Zhang D, Xia Y, Li X. A novel simplified convolutional neural
812 network classification algorithm of motor imagery EEG signals based on deep
813 learning. Applied Sciences. 2020 Jan;10(5):1605. doi: [10.3390/app10051605](https://doi.org/10.3390/app10051605)
- 814 Lotte F, Bougrain L, Cichocki A, Clerc M, Congedo M, Rakotomamonjy A, Yger F.
815 A review of classification algorithms for EEG-based brain–computer

CNN Classification for Motor Imagery BCIs

- 816 interfaces: a 10 year update. Journal of Neural Engineering. 2018 Apr
817 16;15(3):031005. doi: [10.1088/1741-2552/aab2f2](https://doi.org/10.1088/1741-2552/aab2f2)
- 818 Lotte F, Guan C. Regularizing common spatial patterns to improve BCI designs:
819 unified theory and new algorithms. IEEE Transactions on biomedical
820 Engineering. 2010 Sep 30;58(2):355-62. doi: 10.1109/TBME.2010.2082539.
- 821 Lotte F, Faller J, Guger C, Renard Y, Pfurtscheller G, Lécuyer A, Leeb R. Combining
822 BCI with virtual reality: towards new applications and improved BCI.
823 InTowards Practical Brain-Computer Interfaces 2012 (pp. 197-220). Springer,
824 Berlin, Heidelberg.
- 825 Mane R, Robinson N, Vinod AP, Lee SW, Guan C. A Multi-view CNN with Novel
826 Variance Layer for Motor Imagery Brain Computer Interface. In2020 42nd
827 Annual International Conference of the IEEE Engineering in Medicine &
828 Biology Society (EMBC) 2020 Jul 20 (pp. 2950-2953). IEEE. doi:
829 [10.1109/EMBC44109.2020.9175874](https://doi.org/10.1109/EMBC44109.2020.9175874)
- 830 Marchesotti S, Bassolino M, Serino A, Bleuler H, Blanke O. Quantifying the role of
831 motor imagery in brain-machine interfaces. Scientific Reports. 2016 Apr
832 7;6(1):1-2. doi: [10.1038/srep24076](https://doi.org/10.1038/srep24076)
- 833 McFarland DJ, Wolpaw JR. Sensorimotor rhythm-based brain-computer interface
834 (BCI): feature selection by regression improves performance. IEEE
835 Transactions on Neural Systems and Rehabilitation Engineering. 2005 Sep
836 12;13(3):372-9. doi: [10.1109/TNSRE.2005.848627](https://doi.org/10.1109/TNSRE.2005.848627)
- 837 Miao M, Hu W, Yin H, Zhang K. Spatial-frequency feature learning and classification
838 of motor imagery EEG based on deep convolution neural network.
839 Computational and Mathematical Methods in Medicine. 2020 Jul 20;2020.
840 doi: 10.1155/2020/1981728

CNN Classification for Motor Imagery BCIs

- 841 Millán JD, Rupp R, Mueller-Putz G, Murray-Smith R, Giugliemma C, Tangermann
842 M, Vidaurre C, Cincotti F, Kubler A, Leeb R, Neuper C. Combining brain–
843 computer interfaces and assistive technologies: state-of-the-art and challenges.
844 *Frontiers in Neuroscience*. 2010 Sep 7;4:161. doi: 10.3389/fnins.2010.00161
- 845 Müller KR, Krauledat M, Dornhege G, Curio G, Blankertz B. Machine learning
846 techniques for brain-computer interfaces. *Biomed. Tech.* 2004 Dec;49(1):11-
847 22.
- 848 Nicolas-Alonso LF, Gomez-Gil J. Brain Computer Interfaces, a Review. *Sensors*.
849 2012 Feb;12(2):1211-79. doi: [10.3390/s120201211](https://doi.org/10.3390/s120201211)
- 850 Park Y, Chung W. Selective feature generation method based on time domain
851 parameters and correlation coefficients for Filter-Bank-CSP BCI systems.
852 *Sensors*. 2019 Jan;19(17):3769. doi: 10.3390/s19173769
- 853 Pfurtscheller G, Brunner C, Schlögl A, Da Silva FL. Mu rhythm (de) synchronization
854 and EEG single-trial classification of different motor imagery tasks.
855 *NeuroImage*. 2006 May 15;31(1):153-9.
- 856 Pfurtscheller G, Neuper C. Motor imagery and direct brain-computer communication.
857 *Proceedings of the IEEE*. 2001 Jul;89(7):1123-34. doi: 10.1109/5.939829
- 858 Qiao W, Bi X. Deep spatial-temporal neural network for classification of EEG-based
859 motor imagery. In *Proceedings of the 2019 International Conference on*
860 *Artificial Intelligence and Computer Science* 2019 Jul 12 (pp. 265-272). doi:
861 [10.1145/3349341.3349414](https://doi.org/10.1145/3349341.3349414)
- 862 Radiuk PM. Impact of training set batch size on the performance of convolutional
863 neural networks for diverse datasets. *Information Technology and*
864 *Management Science*. 2017 Dec 20;20(1):20-4. doi: [10.1515/itms-2017-0003](https://doi.org/10.1515/itms-2017-0003)

CNN Classification for Motor Imagery BCIs

- 865 Raza H, Cecotti H, Prasad G. Optimising frequency band selection with forward-
866 addition and backward-elimination algorithms in EEG-based brain-computer
867 interfaces. In 2015 international joint conference on neural networks (IJCNN)
868 2015 Jul 12 (pp. 1-7). IEEE. doi: [10.1109/IJCNN.2015.7280737](https://doi.org/10.1109/IJCNN.2015.7280737)
- 869 Robinson N, Lee SW, Guan C. EEG representation in deep convolutional neural
870 networks for classification of motor imagery. In 2019 IEEE International
871 Conference on Systems, Man and Cybernetics (SMC) 2019 Oct 6 (pp. 1322-
872 1326). IEEE.
- 873 Roc A, Pillette L, Mladenovic J, Benaroch C, N'Kaoua B, Jeunet C, Lotte F. A review
874 of user training methods in brain computer interfaces based on mental tasks.
875 Journal of Neural Engineering. 2020 Nov 12. doi: [10.1088/1741-2552/abca17](https://doi.org/10.1088/1741-2552/abca17)
- 876 Roy Y, Banville H, Albuquerque I, Gramfort A, Falk TH, Faubert J. Deep learning-
877 based electroencephalography analysis: a systematic review. Journal of Neural
878 Engineering. 2019 Aug 14;16(5):051001. doi: [10.1088/1741-2552/ab260c](https://doi.org/10.1088/1741-2552/ab260c)
- 879 Saha S, Baumert M. Intra-and inter-subject variability in EEG-based sensorimotor
880 brain computer interface: a review. Frontiers in computational neuroscience.
881 2020 Jan 21;13:87. doi: [10.3389/fncom.2019.00087](https://doi.org/10.3389/fncom.2019.00087)
- 882 Sakhavi S, Guan C, Yan S. Parallel convolutional-linear neural network for motor
883 imagery classification. In 2015 23rd European Signal Processing Conference
884 (EUSIPCO) 2015 Aug 31 (pp. 2736-2740). IEEE. doi:
885 [10.1109/EUSIPCO.2015.7362882](https://doi.org/10.1109/EUSIPCO.2015.7362882)
- 886 Schirrneister RT, Springenberg JT, Fiederer LD, Glasstetter M, Eggenberger K,
887 Tangermann M, Hutter F, Burgard W, Ball T. Deep learning with
888 convolutional neural networks for EEG decoding and visualization. Human
889 brain mapping. 2017 Nov;38(11):5391-420. doi: [10.1002/hbm.23730](https://doi.org/10.1002/hbm.23730)

CNN Classification for Motor Imagery BCIs

- 890 Selim S, Tantawi MM, Shedeed HA, Badr A. A CSP\AM-BA-SVM Approach for
891 Motor Imagery BCI System. IEEE Access. 2018 Aug 31;6:49192-208. doi:
892 10.1109/ACCESS.2018.2868178
- 893 Sharma, S. Epoch vs Batch Size vs Iterations. 2017, September 27. Retrieved from
894 towards data science: [https://towardsdatascience.com/epoch-vs-iterations-vs-](https://towardsdatascience.com/epoch-vs-iterations-vs-batch-size4dfb9c7ce9c9)
895 [batch-size4dfb9c7ce9c9](https://towardsdatascience.com/epoch-vs-iterations-vs-batch-size4dfb9c7ce9c9). [Accessed May 15, 2020]
- 896 Shashibala T, Gawali BW. Brain computer interface applications and classification
897 techniques. International Journal of Engineering and Computer Science.
898 2016;5(7):17260-7.
- 899 Shen Y, Lu H, Jia J. Classification of motor imagery EEG signals with deep learning
900 models. In International Conference on Intelligent Science and Big Data
901 Engineering 2017 Sep 22 (pp. 181-190). Springer, Cham. doi: [10.1007/978-3-](https://doi.org/10.1007/978-3-319-67777-4_16)
902 [319-67777-4_16](https://doi.org/10.1007/978-3-319-67777-4_16)
- 903 Singh A, Lal S, Guesgen HW. Reduce calibration time in motor imagery using
904 spatially regularized symmetric positives-definite matrices based
905 classification. Sensors. 2019 Jan;19(2):379. doi: [10.3390/s19020379](https://doi.org/10.3390/s19020379)
- 906 Škola F, Liarokapis F. Embodied VR environment facilitates motor imagery brain-
907 computer interface training. Computers & Graphics. 2018 Oct 1;75:59-71. doi:
908 [10.1016/j.cag.2018.05.024](https://doi.org/10.1016/j.cag.2018.05.024)
- 909 Stieger J, Engel S, Suma D, He B. Benefits of deep learning classification of
910 continuous noninvasive brain-computer interface control. Journal of Neural
911 Engineering. 2021 May 26. doi: [0.1016/j.cag.2018.05.024](https://doi.org/10.1016/j.cag.2018.05.024)
- 912 Tang Z, Li C, Sun S. Single-trial EEG classification of motor imagery using deep
913 convolutional neural networks. Optik. 2017 Feb 1;130:11-8. doi:
914 [10.1016/j.ijleo.2016.10.117](https://doi.org/10.1016/j.ijleo.2016.10.117)

CNN Classification for Motor Imagery BCIs

- 915 Tayeb Z, Fedjaev J, Ghaboosi N, Richter C, Everding L, Qu X, Wu Y, Cheng G,
916 Conradt J. Validating deep neural networks for online decoding of motor
917 imagery movements from EEG signals. *Sensors*. 2019 Jan;19(1):210. doi:
918 [10.3390/s19010210](https://doi.org/10.3390/s19010210)
- 919 TensorFlow. Overfit and underfit. 2020, July 10. Retrieved from TensorFlow:
920 https://www.tensorflow.org/tutorials/keras/overfit_and_underfit. [Accessed
921 April 02, 2020]
- 922 Thompson MC. Critiquing the concept of BCI illiteracy. *Science and engineering*
923 *ethics*. 2019 Aug;25(4):1217-33. doi: [10.1007/s11948-018-0061-1](https://doi.org/10.1007/s11948-018-0061-1)
- 924 Torres, J. Learning Process of a Neural Network. How Do Artificial Neural Networks
925 Learn? 2020, April 21. Retrieved from towards data science:
926 [https://towardsdatascience.com/learning-process-of-a-deep-neural-network-](https://towardsdatascience.com/learning-process-of-a-deep-neural-network-5a9768d7a651)
927 [5a9768d7a651](https://towardsdatascience.com/learning-process-of-a-deep-neural-network-5a9768d7a651). [Accessed May 05, 2020].
- 928 Ullah I, Manzo M, Shah M, Madden M. Graph Convolutional Networks: analysis,
929 improvements and results. arXiv preprint arXiv:1912.09592. 2019 Dec 19.
- 930 Vidaurre C, Kawanabe M, von Bünau P, Blankertz B, Müller KR. Toward
931 unsupervised adaptation of LDA for brain–computer interfaces. *IEEE*
932 *Transactions on Biomedical Engineering*. 2010 Nov 18;58(3):587-97. doi:
933 [10.1371/journal.pone.0123727](https://doi.org/10.1371/journal.pone.0123727)
- 934 Wang P, Jiang A, Liu X, Shang J, Zhang L. LSTM-based EEG classification in motor
935 imagery tasks. *IEEE transactions on neural systems and rehabilitation*
936 *engineering*. 2018 Oct 18;26(11):2086-95. doi:
937 [10.1109/TNSRE.2018.2876129](https://doi.org/10.1109/TNSRE.2018.2876129)

CNN Classification for Motor Imagery BCIs

- 938 Wang Z, Ma Z, Du X, Dong Y, Liu W. Research on the Key Technologies of Motor
939 Imagery EEG Signal Based on Deep Learning. *Journal of Autonomous*
940 *Intelligence*. 2019;2(4):1-4. doi: 10.32629/jai.v2i4.60
- 941 Wierzgała P, Zapala D, Wojcik GM, Masiak J. Most popular signal processing
942 methods in motor-imagery BCI: a review and meta-analysis. *Frontiers in*
943 *Neuroinformatics*. 2018 Nov 6;12:78. doi: 10.3389/fninf.2018.00078
- 944 Wolpaw JR, McFarland DJ. Control of a two-dimensional movement signal by a
945 noninvasive brain-computer interface in humans. *Proceedings of the National*
946 *Academy of Sciences*. 2004 Dec 21;101(51):17849-54. doi:
947 10.1073/pnas.0403504101
- 948 Yahya N, Musa H, Ong ZY, Elamvazuthi I. Classification of motor functions from
949 electroencephalogram (EEG) signals based on an integrated method comprised
950 of common spatial pattern and wavelet transform framework. *Sensors*. 2019
951 Jan;19(22):4878. doi: 10.3390/s19224878
- 952 Yang H, Sakhavi S, Ang KK, Guan C. On the use of convolutional neural networks
953 and augmented CSP features for multi-class motor imagery of EEG signals
954 classification. In 2015 37th Annual International Conference of the IEEE
955 Engineering in Medicine and Biology Society (EMBC) 2015 Aug 25 (pp.
956 2620-2623). IEEE. doi: 10.1109/EMBC.2015.7318929
- 957 Yuksel A, Olmez T. A neural network-based optimal spatial filter design method for
958 motor imagery classification. *PloS one*. 2015 May 1;10(5):e0125039. doi:
959 10.1371/journal.pone.0125039
- 960 Zapala D, Zabielska-Mendyk E, Augustynowicz P, Cudo A, Jaśkiewicz M, Szewczyk
961 M, Kopiś N, Francuz P. The effects of handedness on sensorimotor rhythm

CNN Classification for Motor Imagery BCIs

- 962 desynchronization and motor-imagery BCI control. Scientific Reports. 2020
963 Feb 7;10(1):1-1. doi: 10.1038/s41598-020-59222-w
- 964 Pérez Zapata AF. Classification of Motor Imagery EEG Signals Using a CNN
965 Architecture and a Meta-heuristic Optimization Algorithm for Selecting
966 Training Parameters.
- 967 Zhang K, Robinson N, Lee SW, Guan C. Adaptive transfer learning for EEG motor
968 imagery classification with deep Convolutional Neural Network. Neural
969 Networks. 2021 Apr 1;136:1-0. doi: [10.1016/j.neunet.2020.12.013](https://doi.org/10.1016/j.neunet.2020.12.013)